

FTUV/IFIC-9832
hep-ph/9807371

Neutrino Spin Flavour Precession in Fluctuating Solar Magnetic Fields.

E. Torrente-Lujan.

Dpto. Fisica Teorica, Universitat de Valencia.

Dr. Moliner 50, E-46100 Burjassot, Valencia.

e-mail: e.torrente@cern.ch

Abstract

The effect of a random magnetic field in the convective zone of the Sun on resonant neutrino spin oscillations, i.e. transitions of the type $\nu_{eL} \rightarrow \tilde{\nu}_{\mu R}$, is considered. The average survival probability and the expected experimental signals in the existing solar neutrino experiments are computed as a function of the level of the noise and magnitude of a constant magnetic field in the convective zone. From comparison with observed detection rates we conclude that the RSFP solutions to the SNP with negligible mixing angle are stable under the presence of low or moderate levels of noise. Detection rates, specially in the Homestake experiment, are however sensitive to large levels of noise. As a consequence, an upper limit on small scale magnetic fluctuations is obtained from the combined solar data: $\sqrt{\langle B^2 \rangle} < 140 - 200$ kG for the scale $L_0 \sim 1000$ km and transition moment $\mu = 10^{-11} \mu_B$.

1. A neutrino transition magnetic moment can account, as it has been shown in ([1]), for both the observed deficiency of the solar neutrino flux and the possible time variations of the signal. The overall deficit is caused by the alteration or suppression of the neutrino energy spectrum. The time dependence may be caused by time variations of the magnetic field in the convective zone of the Sun.

The two main problems for the RSFP scenario are the large size of neutrino magnetic moment which is needed and the scarce knowledge which is available on the structure of the magnetic field inside the Sun. To overcome the second problem, authors usually consider different “plausible” radial magnetic field profiles. The absence of a strong poloidal field around the Sun limit strongly the maximum value of the magnitude of a magnetic field in its inner parts. Therefore, a zero magnetic field is usually considered for the solar core. In the convective zone, fields of the order of a few kG up to a few tens of kG are usually considered possible.

In this article we will address another aspect of the RSFP scenario: the nature of the magnetic field. Magnetic fields in nature are very often stochastic or at least strongly chaotic. This happens both, when considering the magnetic fields coming from the seeding of primordial fields or more mundane fields such as those present in the external shell of the Sun. Neutrino propagation in a medium with random magnetic fields has special properties, differentiated from the situation where only regular magnetic fields are present. The effective Hamiltonian governing the evolution of averaged quantities become non-hermitic and some sort of dissipation is introduced. Average conversion probabilities become aperiodic and more sensitive to vacuum parameters in some cases. It has been shown for example that limits on magnetic moments derived including random magnetic fields in Supernova are stronger than those derived using only regular fields (see [2]). On the other hand, for strong noise the situation is in some sense opposite, as we will see below in this work the survival probability approaches one half irrespective of the value of the vacuum parameters.

The aim of this letter is to study the effect of the introduction of a random magnetic component in a simple RSFP scenario: one which disregards neutrino mixing and assumes that the direction of the transverse field does not change along the neutrino trajectory. It has been shown ([3]) that the same model with a regular magnetic field profile can provide a rough solution to the SNP. The conclusion of [3] is that all the available solar neutrino data can be fitted for $\Delta m^2 \sim 2 \times 10^{-8} - 4 \times 10^{-9} \text{ eV}^2$ with no inner field and a convective-zone magnetic field varying between $2.5 - 5 \times 10^4 \text{ G}$ ($\mu = 10^{-11} \mu_B$).

Summarily, the main advantages of models including random magnetic fields are connected with: a) The no necessity to know in detail specific magnetic profiles. b) The potentially stronger effect of the random magnetic field in comparison to regular magnetic field: for the latter the spin precession is roughly proportional to the quantity $\exp C \int dr B(r)$ where the integral is extended over the region where the magnetic field B is present. However for the case of random magnetic fields the precession is proportional to $\exp C' \int dr B^2(r)$. In addition the chaotic precession is irreversible and regeneration effects of the original neutrino flux are absent or reduced. c) It is still important to assume

a large transition magnetic moment μ for the neutrino, but the dependence on it is substantially altered. While for regular oscillations the constant $C \sim \mu$, for random magnetic fields $C' \sim \Omega^2 L_0 \mu^2$. The dependence on the magnetic moment μ can be traded off, at least partially, for the dependence on the parameters Ω^2, L_0 . These parameters describe the randomness and the coherence length of the magnetic field, they can be potentially very large, with an accepted range of variation of $\sim 1 - 3$ orders of magnitude. d) The overall influence of the random nature of the magnetic field is the flattening of the neutrino spectrum. The strong energy dependence on resonances is reduced, so this scenario is a natural way to avoid strong time variations.

The structure of the article is as follows. First we will write the basic neutrino propagation equations in presence of matter and magnetic field. In the next section a brief description of the corresponding evolution equation for the averaged density matrix (the Redfield equation) is given. Finally the last section is dedicated to show the results of the numerical calculations and concluding remarks: The Homestake, SAGE-GALLEX (Ga-Ge) and (Super)-Kamiokande expected signal rates has been calculated and compared with available experimental observations.

2. Taking into account theoretical and observational evidence of the solar surface and convection region magnetic fields it is expected ([4, 5]) that the neutrino, while traveling through the convection zone, will encounter a magnetic field of complicated unknown structure which will be the sum of large and small (fluctuating) scale components of sufficiently large amplitude and short correlation length. In this work, we will approximate such a field by the simplest possible expression:

$$B(t) = B_0 + \tilde{B}(t) \quad (1)$$

where B_0 is a *constant* magnetic field over the full extent of the convective zone. $\tilde{B}(t)$ is a fluctuating field with zero average acting over a relative small layer at the bottom of the convective zone (the unstable transition region between $r \approx 0.65 - 0.75 R_0$). It is assumed that $\tilde{B}(t)$ is a stochastic field: a zero-average δ -correlated Gaussian process characterized by a two-point correlation function parametrized as follows:

$$\langle \tilde{B}(t) \tilde{B}(t') \rangle = \langle \tilde{B}^2 \rangle L_0 \delta(t - t') = \eta B_0^2 L_0 \delta(t - t'). \quad (2)$$

The length L_0 is a basically unknown parameter, values in the range $10^3 - 10^4$ should be allowed. It has been shown in [6] that the δ -correlation function is a sufficiently good approximation to more realistic finite correlators even for relative large correlation lengths. The coefficient η is the ratio between large and small scale fields: it is estimated ([4], p. 517; see also [5]) by the expression

$$\eta \simeq \frac{1}{\epsilon} \frac{v}{V_0} \quad (3)$$

where V_0 corresponds to the Alfvén speed in the large scale field B_0 , v is the turbulent fluid velocity and ϵ is a, model dependent, undetermined number smaller than one. In the

turbulent dynamo theory the magnetic field is carried in the plasma; equating magnetic and kinetic energy, we obtain $v \approx V_0$, and so $\eta > 1$. Some other estimations favor much higher values $\eta \gg 1$ ([7]).

In transverse magnetic fields, neutrinos with transition magnetic moments will experience spin and flavour rotation simultaneously. For Majorana neutrinos the RSFP converts left-handed neutrinos of a given flavour into right-handed neutrinos of a different flavour. Disregarding flavour neutrino mixing by simplicity the evolution of two Majorana neutrinos $(\nu_{eL}, \bar{\nu}_{\mu R})$ in presence of matter and magnetic fields is described by the following effective Hamiltonian:

$$i \frac{d}{dt} \begin{pmatrix} \nu_{eL} \\ \bar{\nu}_{\mu R} \end{pmatrix} = \begin{pmatrix} V - \Delta & \mu B_{\perp}^- \\ \mu B_{\perp}^+ & 0 \end{pmatrix} \begin{pmatrix} \nu_{eL} \\ \bar{\nu}_{\mu R} \end{pmatrix} \quad (4)$$

where

$$B_{\perp}^{\pm}(t) \equiv B_x(t) \pm i B_y(t) \equiv |B_{\perp}(t)| e^{\pm i \Phi(t)} \quad (5)$$

and

$$\Phi(t) = \arctan B_y/B_x. \quad (6)$$

The matter potential is $V = \sqrt{2}G_F(N_e - N_n)$ where N_e, N_n are the electron and neutron number densities, G_F is the Fermi constant and $\Delta = \Delta m^2/2E$. The magnetic field strength B enters the evolution Eq.(4) being multiplied by the neutrino transition moment μ . The existing upper limits on the magnetic moment of the electron neutrino include the laboratory bound $\mu < 2 \times 10^{-10} \mu_B$ from reactor experiments as well as stronger (one or two orders of magnitude) astrophysical and cosmological limits. Expected values of $B \approx 1 - 100$ kG in the Sun convective zone and $\mu = 10^{-11} \mu_B$ would give an expected range for the product $\mu B \approx 10^{-8} - 10^{-6} \mu_B G \approx 5.6 \cdot 10^{-7} - 10^{-15}$ eV or in the practical units which will be used throughout this work $\mu B \approx 0.1 - 10 \mu_{11} B_4$.

Assuming that the direction of the transverse magnetic field does not change along the neutrino trajectory (absence of twist) the evolution equation can be written as:

$$i \frac{d}{dt} \begin{pmatrix} \nu_{eL} \\ \bar{\nu}_{\mu R} \end{pmatrix} = \begin{pmatrix} V - \Delta & \mu B_{\perp} \\ \mu B_{\perp} & 0 \end{pmatrix} \begin{pmatrix} \nu_{eL} \\ \bar{\nu}_{\mu R} \end{pmatrix}. \quad (7)$$

In the case of constant magnetic field and matter density, the corresponding transition probability obtained from Eq.(7) is

$$P(\nu_{eL} \rightarrow \bar{\nu}_{\mu R}) = \sin^2(k\mu B_{\perp} t)/k^2 \quad (8)$$

with $k^2 = 1 + (\Delta - V)^2/(\mu B_{\perp})^2$. In resonance ($\Delta \sim V$) or for strong μB_{\perp} the constant $k \sim 1$ and the probability is a periodic function of B with maximum amplitude ~ 1 .

The problem described by Eq.(7) when V is locally varying and B is a *constant* is formally equivalent to a MSW problem with a pseudo mixing angle given by a certain function of Δ and μB . In the presence of a matter density of exponential profile, as approximately happens in the solar case, and a constant transverse field, the precession probability can be obtained in a closed analytic form (see [8] for a two generation case, [9]

for a general case). In this case the evolution matrix for the solution to Eq.(4) is given by (detailed expressions can be found in [9]):

$$U(t, t_0) = U_s^\dagger(t) U_s(t_0), \quad U_s(t) = \exp(iH_0 t) U_r(t). \quad (9)$$

The Hamiltonian H_0 and effective mixing matrix u are

$$H_0 = u \begin{pmatrix} \lambda_+ & 0 \\ 0 & \lambda_- \end{pmatrix} u^\dagger; \quad u = \begin{pmatrix} \cos \theta & -\sin \theta \\ \sin \theta & \cos \theta \end{pmatrix} \quad (10)$$

With $\lambda_\pm = \Delta \left(-1 \pm \sqrt{1+e^2} \right) / 2$; $e = 2\mu B_\perp / \Delta$, $\tan^2 \theta = -\lambda_- / \lambda_+$. The elements of the matrix U_r are simple analytic functions of Δ, V and the “mixing angle” θ .

3. The master Equation (4) can be written in terms of the corresponding 2x2 density matrix $\rho(t)$ as:

$$i \frac{d\rho}{dt} = [H_{reg}, \rho] + \mu \tilde{B}_x(t) [\sigma_1, \rho] + \mu \tilde{B}_y(t) [\sigma_2, \rho]. \quad (11)$$

The \tilde{B}_x, \tilde{B}_y are the Cartesian transversal components of the chaotic magnetic field. Vacuum mixing terms, matter terms corresponding to the SSM density profile and the regular magnetic part Hamiltonian, are all included in H_{reg} . $\sigma_{1,2}$ are the standard Pauli matrices.

We assume that the components \tilde{B}_x, \tilde{B}_y are statistically independent, each of them characterized by a δ -correlator. The averaged evolution equation is a simple generalization (see [6] for a complete derivation) of the well known Redfield equation ([10]) for two independent sources of noise and reads ($\Omega^2 = \mu^2 \langle \tilde{B}^2 \rangle L_0$):

$$i \frac{d\langle \rho \rangle}{dt} = [H_{reg}, \langle \rho \rangle] - i\Omega^2 ([\sigma_1, [\sigma_1, \langle \rho \rangle]] + [\sigma_2, [\sigma_2, \langle \rho \rangle]]). \quad (12)$$

Eq.(12) can be also written as:

$$i \frac{d\langle \rho \rangle}{dt} = [H_{reg}, \langle \rho \rangle] - 2i\Omega^2 (2\langle \rho \rangle - \sigma_1 \langle \rho \rangle \sigma_1 - \sigma_2 \langle \rho \rangle \sigma_2). \quad (13)$$

In the averaged evolution equations the length L_0 appears only through the product ηL_0 . Therefore, we will present our results as a function of the quantity P which is a simple function of such a product:

$$\begin{aligned} P &= \frac{1}{2} (1 + \exp(-\gamma)), \\ \gamma &\equiv 4\Omega^2 \Delta t \equiv 4\eta L_0 (\mu B_0)^2 / 3. \end{aligned} \quad (14)$$

One reason for using P is that it is a good approximation for the depolarization that the presence of noise induces in the averaged neutrino density matrix. Δt is the distance over which the noise is acting.

In general Eq.(13) must be solved numerically. For that purpose we have found advantageous to reduce such equation to a single integral equation. The procedure, which could be of some interest for other applications, is outlined in the appendix.

4. We have supposed in our numerical calculation that the noise is effective only in a thin layer with thickness $\Delta t = 0.1 R_\odot$ starting at $r = 0.65 R_\odot$. Different levels of noise are parametrized by the quantity P (Eq.(14)) which varies between 1 (no noise) and $1/2$ (maximal noise). This equivalent to a range for the r.m.s field $\sqrt{\langle \tilde{B}^2 \rangle} \sim 0 - 600$ kG (assuming the reasonable value of the length $L_0 = 1000$ Km and $\mu = 10^{-11} \mu_B$).

Fig.(1) shows the distortion of the neutrino energy spectrum for different levels of noise. We plot the survival probability for an electron neutrino created at the solar interior when arriving at the Earth. The neutrino travels in a constant magnetic field of magnitude, in this example, $\mu B = 4.0 \mu_{11} B_4$ along all the convective zone. An exponential profile as given by [11] is used for the matter density. This plot has been obtained using the exact solution (Eqs.(9)) for the noiseless case and the numerical solution to Eq.(24) for the non-zero noise cases. Numerical integration of the original differential equations gives the same results, at a much more higher CPU cost.

The squared mass difference used in Fig.(1) is $\Delta m^2 = 5.0 \times 10^{-9}$ eV 2 . This value implies that some RSFP occurs at the relevant neutrino energies: For the RSFP to be effective in the convective zone it is necessary that $\Delta m^2/2E < 10^{-7}$ eV 2 /MeV, or for the typical solar energies $\Delta m^2 < 10^{-8}$ eV 2 . It is clear from Fig.(1) that the lowest-energy pp-neutrinos with characteristic energy $E_{pp} \approx 0.3$ MeV, which are detected only in the Ga-Ge detectors (where they provide more than half of the signal) are hardly affected by the magnetic field. Intermediate and higher energy neutrinos are strongly suppressed. When noise is applied the distortion tends to disappear and the spectrum becomes practically flat over all the energy range considered (for $P < 0.7 - 0.8$). One important observation from the figure is that the influence of the noisy magnetic field is significant for all values of Δm^2 even for those whose resonance point is not exactly in the region where the chaotic field is present.

In the next figure, Fig.(2), we show the expected signal rates in different neutrino experiments. The ratio of the averages of the observed detection rates and the SSM expected rates which have been used are shown below (1σ statistical and systematic combined errors,[12]; the SSM predictions are those of [11]): Homestake 0.27 ± 0.027 , SuperKamiokande (345 days) $0.375^{+0.040}_{-0.002}$, Ga-Ge (SAGE-GALLEX combined) 0.51 ± 0.06 . For computing the expected signal at the Kamiokande experiment we have taken into account the two elastic scattering processes $\nu_x e \rightarrow \nu_x e$ with $\nu_x = \nu_e, \bar{\nu}_\mu$. We have used the expressions for the elastic cross sections appearing in [13] with a kinetic energy threshold for the observation of the scattered electron of $T_{e,min} \sim 7$ MeV.

We observe that the signal is successively correlated (situation not favored from the data) or anti-correlated with the value of the magnetic field. The periodic structure of the plots is explained easily if we take into account Eq.(8). The variation for the Ga-Ge experiments is always significantly lower than those for Kamiokande or Homestake as it could be expected from the previous discussion about the energy spectrum distortion. The introduction of noise smoothes the amplitude of the periodic variations ¹.

In Fig.(3) we present the single and combined χ^2 exclusion plots corresponding to the

¹ Of course we could also think of time variations induced by a modulated P .

expected signal rates at the three experiments as a function of the oscillation parameter, regular magnetic field and fluctuation amplitude. The Akhmedov ([3]) solutions are reproduced clearly ($\Delta m^2 \approx 10^{-8}$ eV 2 , $\mu B \approx 4 \mu_{11} B_4$ and higher modes). These solution regions (shaded areas) do not change with the addition of noise up to a value $P = 0.8$. For the value $P = 0.7$ we observe that the solution with the lower magnetic field has disappeared already. For values $P < 0.7$ (not shown in the plot) the three allowed regions from combined data disappear completely.

If we observe the outcome of the individual experiments (individual lines) we can conclude that the stronger constraint at high noise comes from the Homestake data. The other two experiments show contradictory tendencies which can be explained by the different weight of the different parts of the neutrino spectrum in each of them. While the Kamiokande allowed region tends to shrink with increasing noise, the region allowed by the Ga-Ge data in fact enlarges to a maximum extension. At $P = 0.7$ and low magnetic field there is a large common area which is allowed by both Kamiokande and Ga-Ge data.

Taking into account the three experiments, and within this very simple scenario, particle physics solutions to the solar neutrino problem are allowed only if $P > 0.8 - 0.7$. According to the figures, stronger values of the noise are still allowed if we admit solutions with ever larger magnetic fields. Large magnetic fields in the convective zone are, if not completely discarded, at least disfavored by astrophysics. However from the purely neutrino experimental side these solutions increase in attractiveness in conjunction with large noise because of the (anti)-correlation smoothening observed in Fig.(2).

In conclusion we have shown that RSFP solutions to the solar neutrino problem with negligible neutrino mixing survive in the presence of random magnetic fields of low or moderate level ($P > 0.8 - 0.7$, or $\sqrt{\langle B^2 \rangle} < 140 - 200$ kG for $\mu = 10^{-11} \mu_B$ and a fluctuating scale $L_0 = 1000$ km). Conversely, by requiring a particle solution to the solar neutrino problem, in the proposed scenario this range of values for P can be interpreted as a upper limit on the presence small scale fluctuating magnetic fields in the solar convective zone. According to [6] the δ -correlation function is a sufficiently good approximation to more realistic finite correlators even for relative large correlation length. Moreover, the quantity P is connected with the depolarization of the density matrix. It offers some advantage with respect to more "physical" parameters as Ω^2 or $\sqrt{\langle \tilde{B}^2 \rangle}$: we expect that results expressed in terms of P are largely independent of the concrete modelizing of the stochastic properties of the fluctuating field (in particular the form of the correlator). Additional, potentially stronger, restrictions on the level of noise can be expected when considering the experimental bounds in the solar antineutrino flux from Kamiokande and the next generation of solar experiments.

Appendix

Our objective in this appendix is to introduce some mathematical manipulations in order to obtain an equation adequate for the purpose of numerical calculation. As a preliminary step, a term can be eliminated from Eq.(13) if we define a new density $\langle \rho_A(t) \rangle$

as:

$$\langle \rho \rangle \equiv e^{-4\Omega^2(t-t_0)} \langle \rho_A(t) \rangle. \quad (15)$$

It is convenient in addition to define a vector representation for the density matrix ρ ; we define, using the standard Stokes parameters:

$$\rho = \text{Diag}((\rho_{11} - \rho_{22}), 2\Re \rho_{12}, 2\Im \rho_{12}).$$

In vectorial form, the equation (12) is:

$$i \frac{d\langle \rho_A \rangle}{dt} = (H_{reg}^V - 8i\Omega^2\tau_1) \langle \rho_A \rangle, \quad (16)$$

where H_{reg}^V and τ_1 are 3×3 matrices. In particular τ_1 , which is vectorial equivalent to $\sigma_1^2 + \sigma_2^2$, is of the form $\tau_1 = i \text{Diag}(1, 0, 0)$.

Our strategy will be to solve exactly the problem corresponding to the first term of the Hamiltonian in Eq.(16) and to consider the second one as a perturbation. We will be able to sum the infinite terms of the perturbative series in terms of a single unknown-function to be defined later. This unknown function is the solution of a certain scalar integral equation. We have found this procedure, albeit apparently artifcious, very advantageous in practical computations.

Let be $U^0(t, t_0)$ the evolution matrix corresponding to the equation:

$$i \frac{d\langle \rho_A \rangle}{dt} = H_{reg}^V \langle \rho_A \rangle \quad (17)$$

for the solar matter exponential density profile and for $B(t) = B_0$, a constant. This equation can be solved exactly (see Eqs.(9-10)). Let us consider now the evolution matrix U for the full equation Eq.(16) and its interaction representation counterpart U_I given by:

$$U_I(t, t_0) = U^{0\dagger}(t, t_0)U(t, t_0). \quad (18)$$

Our main result, which can be proved easily, is that the elements of U_I are given by the following exact formula:

$$U_I(t, t_0)_{ij} = \delta_{ij} + (-i\Omega^2) \int_{t_0}^t dt_1 A_i(t_1) S_j(t_1). \quad (19)$$

The vector S is the solution of the following integral equation with kernel K :

$$S(t) = B(t) + (-i\Omega^2) \int_{t_0}^t dt_1 K(t, t_1) S(t_1). \quad (20)$$

The vectors A, B are defined as

$$A_i(t) \equiv U_{i,1}^{0\dagger}(t, t_0); \quad B_i(t) \equiv U_{1,j}^0(t, t_0); \quad (21)$$

the kernel K is

$$K(t_1, t_2) \equiv \sum_l B_l(t_1) A_l(t_2) \quad (22)$$

In symbolic form the solution to Eq.(20) can be written as:

$$S = (1 + i\Omega^2 K)^{-1} B, \quad (23)$$

the solution to Eq.(19) is then, in the same symbolic form,

$$U_I = 1 + (-i\Omega^2) \int A (1 + i\Omega^2 K)^{-1} B \quad (24)$$

This is the concrete equation which has been used as the basis for numerical computations.

Acknowledgments.

I am grateful to V.B. Semikoz for many and very useful discussions about the nature of the solar magnetic fields.

References

- [1] E.K. Akhmedov. IC/97/49. *Invited talk at the 4th Intl. Solar Neutrino Conference, Heidelberg, Germany, April 8-11, 1997*
- [2] S. Pastor, V.B. Semikoz, J.W.F. Valle. Physics Letters **B369** (1996) 301-307.
- [3] E.K. Akhmedov, A. Lanza, S.T. Petcov. Phys. Lett. **B303** (1993), pp. 85-94.
- [4] E. N: Parker. *Cosmical Magnetic Fields*. Clarendon Press, Oxford, 1979.
- [5] A. Nicoladis. Phys. Lett. **262** (1991) 2,3, pp. 303-306.
- [6] E. Torrente-Lujan. hep-ph/9807361.
- [7] E. Torrente-Lujan, V.B. Semikoz.. Work in preparation.
- [8] S.T. Petcov. Phys. Lett. **B200** (1988) 373..
- [9] E. Torrente-Lujan. Phys. Rev. **D53** (1996), pp. 53-67.
- [10] F.N. Loret, A.B. Balantekin. Phys. Rev. **D50** (1994), pp. 4762-4770.
- [11] J.N. Bahcall and M.H. Pinsonneault, Rev. Mod. Phys. **67** (1995) 781.
- [12] V. Berezinsky. astro-ph/9710126.
- [13] S. Pastor, V.B. Semikoz, J.W.F. Valle. Phys. Lett. **B423** (1998) 118-125.

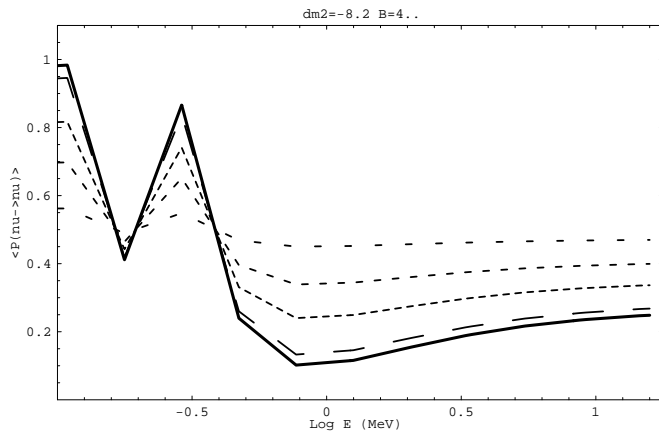


Figure 1: Distortion of the neutrino energy spectrum for different levels of noise: $P = 1.00$ (no noise, solid line); $P = 0.95, 0.80, 0.70, 0.50$ (consecutive dashed lines). The equivalent values for $\sqrt{\langle \tilde{B}^2 \rangle}$ are respectively $0.0, 70, 150, 200, 600$ kG (supposing a scale $L_0 = 1000$ Km, $\mu = 10^{-11} \mu_B$ and a noise region width $\Delta t = 0.1 R_\odot$). The corresponding values for the ratio η are $\eta \equiv \langle B^2 \rangle / B_0^2 = 0, 3, 14, 25, 225$. It has been used the parameters $\Delta m^2 = 5.0 \cdot 10^{-9} eV^2$ and $\mu B_0 = 4.0 \mu_{11} B_4$.

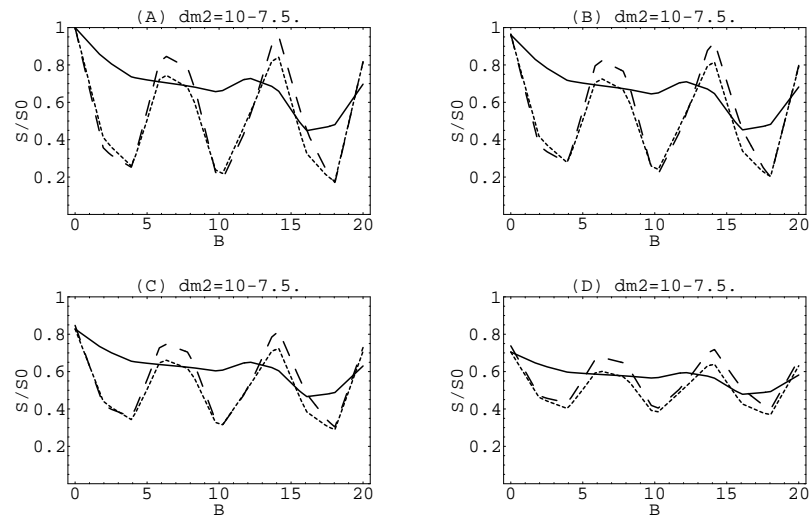


Figure 2: The ratio S/S_0 (theoretical over observed signal rates) as a function of the magnetic field for the three solar neutrino experiments: Combined Ga-Ge (solid line), SuperKamiokande (long dashed line) and Homestake (dotted line). $\Delta m^2 = 3 \times 10^{-8} \text{ eV}^2$. Plot(A), $P=1$ (absence of noise). Plots (B,C,D), $P=0.95, 0.8, 0.7$ respectively (see caption in Fig.(1)).

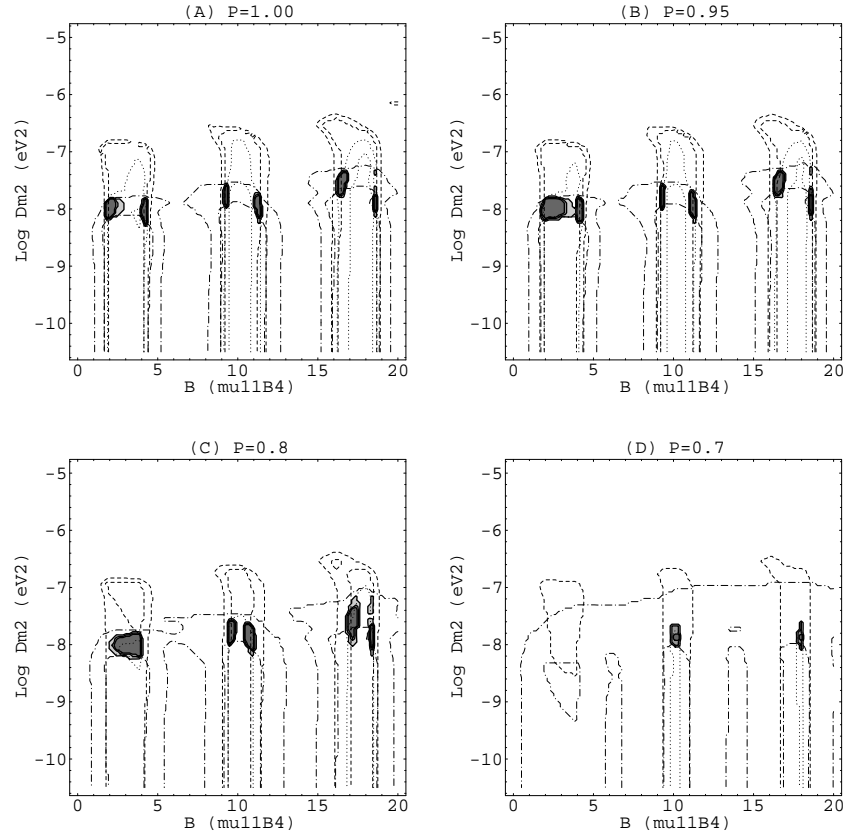


Figure 3: Parameter space regions consistent with the observations at the three neutrino experiments. From light to darker shaded areas combined χ^2 90,95,99% C.L. intervals. Lines refer to individual experiments (95% C.L.): Homestake (dotted line), Ga-Ge (dot-dashed), Kamiokande (dashed). Plot (A), $P=1$ (absence of noise). Plots (B,C,D), $P=0.95, 0.8, 0.7$. (See caption in Fig.(1)).